iScience

CellPress
OPEN ACCESS

Article

Short heat shock has a long-term effect on mesenchymal stem cells' transcriptome

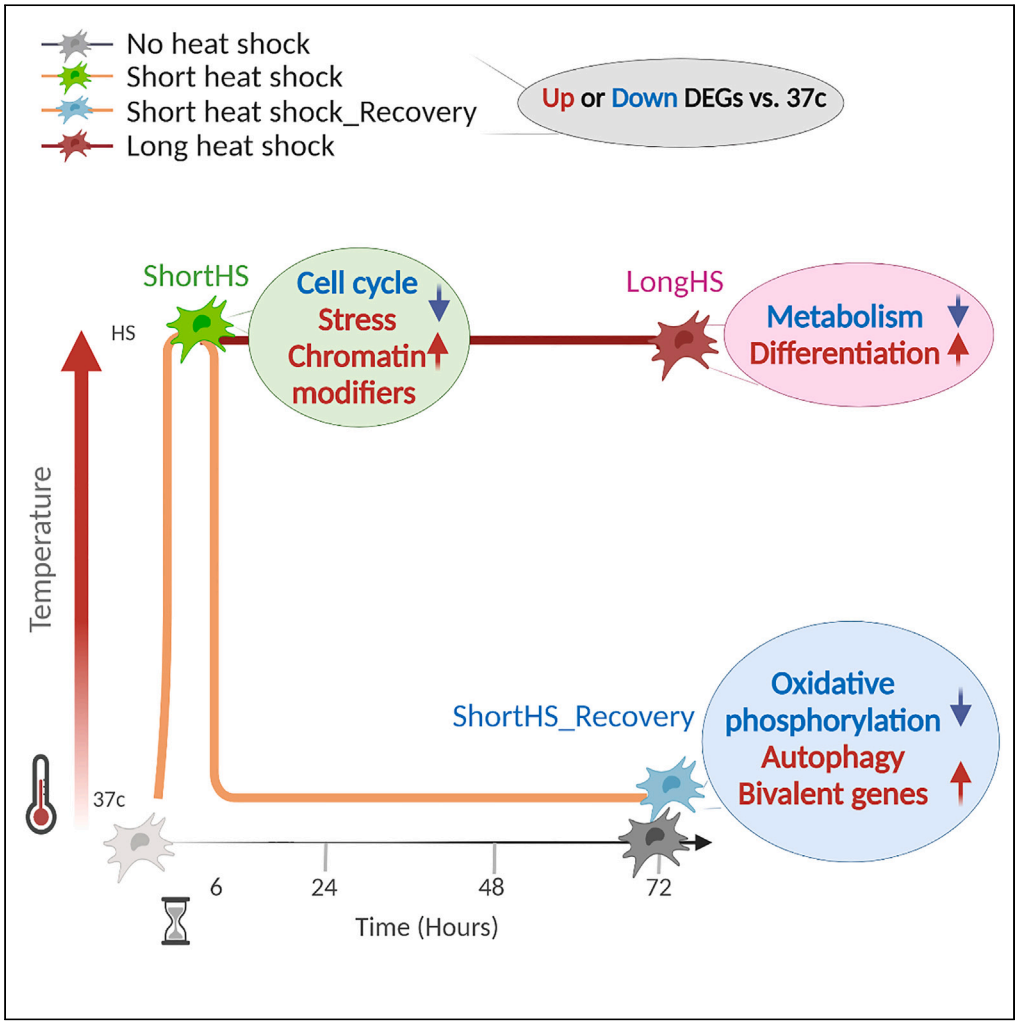

Ivana Ribarski-Chorev, Gisele Schudy, Carmit Strauss, Sharon Schlesinger

sharon.shle@mail.huji.ac.il

Highlights

Heat shock changes MSCs transcriptome, affecting proliferation and fate determination

Short heat shock causes lasting effects on the cells' epigenetic regulation

Upregulation of developmental bivalent genes was observed 72 h after heat shock

Ribarski-Chorev et al., iScience 26, 107305
August 18, 2023
https://doi.org/10.1016/j.isci.2023.107305

iScience

CellPress
OPEN ACCESS

Article

Short heat shock has a long-term effect on mesenchymal stem cells' transcriptome

Ivana Ribarski-Chorev,[1] Gisele Schudy,[1] Carmit Strauss,[1] and Sharon Schlesinger[1,2,*]

SUMMARY

The adverse effects of heat stress (HS) on physiological systems are well documented, yet the underlying molecular mechanisms behind it remain poorly understood. To address this knowledge gap, we conducted a comprehensive investigation into the impact of HS on mesenchymal stem cells (MSCs), focusing on their morphology, phenotype, proliferative capacity, and fate determination. Our in-depth analysis of the MSCs' transcriptome revealed a significant influence of HS on the transcriptional landscape. Notably, even after a short period of stress, we observed a persistent alteration in cell identity, potentially mediated by the activation of bivalent genes. Furthermore, by comparing the differentially expressed genes following short HS with their transcriptional state after recovery, we identified the transient upregulation of MLL and other histone modifiers, providing a potential mechanistic explanation for the stable activation of bivalent genes. This could be used to predict and modify the long-term effect of HS on cell identity.

INTRODUCTION

Environmental stressors harm human and animal health around the world.[1,2] Heat exposure is an increasing problem as climate change progresses; exposures to extreme temperatures vastly affect the organism as a whole and on the cellular level. Adverse effects of heat stress (HS) in humans include heat stroke, systemic inflammation, nervous system impairment, adverse birth outcomes, global DNA methylation, and telomere shortening.[1] In animals, HS was found to have detrimental effects on fertility and well-being.[3–5] In cattle, the frequency of many chronic inflammation-related diseases is elevated during hot periods,[6,7] resulting in reduced animal welfare and significant economic losses to the dairy industry.[8] *In-utero* HS in cattle was recently found to reduce placental weight, blood flow, birth weight, and innate and cellular immunity.[9] Moreover, HS has a long-term effect on oocyte developmental capacity and follicular steroidogenesis in cattle and other mammals.[10,11] It has been suggested that alterations in the cellular epigenetic landscape are responsible for these persisting effects.[5,12,13]

On a cellular level, thermal stress is associated with oxidative stress, endoplasmic reticulum (ER) stress, and neurochemical stress and impairs protein folding, cell cycle, and mitochondrial function.[3,4,14,15] On the transcriptional level, cells exposed to HS generally activate a cascade of heat shock proteins and factors which, in turn, regulate downstream pathways that protect the stressed cells. The effect of external temperature has been examined in various animals and tissues such as bovine peripheral blood mononuclear cells,[16] mammary tissues[17,18] and granulosa cells.[19] Another study exposed rats to HS and examined the transcriptional changes in 3 different tissues.[20] Although many key genes and pathways that respond to acute thermal stress were identified in these studies, only a few genes were common across tissues, suggesting a high level of tissue specificity in the transcriptional response to thermal stress.

HS effects on adult stem cells are of special interest. These cells are the longest-living proliferative cells in multicellular organisms[21]; hence they have an increased risk of accumulating genetic and metabolic damage. Extrinsic factors, including environmental stress, can enhance this damage accumulation, possibly leading to the functional decline of the stem cells.[22] Mesenchymal stromal cells (also called mesenchymal stem cells, MSCs) are a heterogeneous group of non-hematopoietic multipotent stem cells that assist in the preservation of homeostasis in many organs and tissues.[23] Additionally, physiological MSC stores are essential for the regeneration of many tissues in the body, acting through common signaling pathways such as Wnt, BMP, and Notch.[24] Cultured MSCs are most frequently derived from adult tissue sources

[1]The Robert H. Smith Faculty of Agriculture, Food and Environment, The Hebrew University of Jerusalem, Rehovot 7610001, Israel

[2]Lead contact

*Correspondence: sharon.shle@mail.huji.ac.il

https://doi.org/10.1016/j.isci.2023.107305

such as bone marrow and adipose tissue or from birth-associated tissue such as placental tissue, amniotic membranes, and umbilical cord.[25,26] When grown in culture, MSCs can self-renew, differentiate into several tissues, and modulate the immune response in their surroundings.[27–29] When activated, MSCs secrete biologically active compounds and generate exosomes that modify the function of their cellular microenvironment.[30–32] Due to these characteristics, MSCs are commonly suggested as candidates for cell-based therapy or as the cell source for tissue engineering and cultured meat products. However, it is still unclear how the properties and key biological functions of MSCs *in vitro* are influenced by parameters such as cell source, culture conditions, and environmental factors, including HS. Indeed, the long-term epigenetic effects of variations in culture conditions are only beginning to be uncovered.[12,33] An example of such an effect is hypoxia-preconditioning, which was shown to significantly reduce global 5hmC in swine MSCs but had no effects on H3K4me3, H3K9me3, or H3K27me3.[33] Overall, the long-term effects of stress on MSCs are barely characterized.

Here, we evaluated HS treatment's immediate and long-term effects on the bovine umbilical cord (bUC)-derived MSC transcriptome. Our previous study demonstrated that HS treatment changed the proliferation, differentiation, and immunomodulatory potential of bUC-MSCs.[15] Several HS protocols were shown to have the common effect of reducing proliferation and inducing oxidative stress and premature senescence. However, each HS protocol showed profound variation in gene expression and immunomodulatory potential. Surprisingly, even 1 h of treatment at 42°C had a long-term effect on bUC-MSCs function and transcriptional pattern three days after the HS, which partially persisted even after eleven passages (about 40 days) in culture.[15] However, at temperatures higher than 41°C, the survival rate of mammalian cells decreases with increasing exposure time.[34,35] Here, to gain an unbiased view of the cell-intrinsic response to heat shock, we performed gene expression profiling using RNA sequencing (RNA-Seq) following exposure of the bUC-MSCs to moderate HS (40.5°C) of different lengths. We hypothesize that transcriptional response to HS has two manifestations: a major immediate and transitory reaction of stress response-related genes and a minor but permanent response of epigenetically altered transcripts. By examining the transcriptional response and functionality of MSCs after mild HS, this work will advance our understanding of thermal stress's short- and long-term impacts on the organismal stem cell pool.

RESULTS

RNA-seq analysis of heat shock treated and control cells

To examine the effects of thermal stress on the cell's transcriptome, we evaluated the transcriptional response of MSCs to *in vitro* heat shock (HS). MSCs were extracted from the UC of a preterm fetus as previously described.[15] In addition, prior to the HS treatment, MSCs marker expression (Figure S1A), proliferation (Figure S1B), and differentiation capacities (Figure S1C) were examined and validated as in.[15,36]

HS treatment protocols were designed to examine the short- or long-term effects of exposure to mild HS conditions (Figure 1A). One day after seeding MSCs from early passages (P2–P4) were moved from 37°C to 40.5°C for 6 h (ShortHS) or three days (LongHS) or a 6-h HS followed by three days of recovery back at 37°C (ShortHS_Recovery). Each HS treatment had a matching 37°C normothermic (NT) control (ShortNT and LongNT). Two or three biological repeats were done for each treatment (Table S1). The two time points were selected to capture the immediate transcriptional effects of HS vs. the stable and delayed ones. Immediately after the completion of the 6 h or three-day treatments, the cells were harvested, viability was checked, and pellets were stored at −80° for later matched RNA extraction and sequencing. The cells' viability and MSC marker expression levels remained high following the various treatment protocols (Figures S1A and S1D). All RNA samples were run together on NextSeq Illumina and showed a high percentage and quality of mapping to exons and low levels of rRNA and mitochondrial DNA contaminations (Figure S2A and Table S1). Principal component analysis shows that the HS treatment determined the transcriptome profile as samples from the same treatment clustered together and apart from the other treatment groups (Figure 1B). Hierarchical clustering uncovered a secondary factor affecting the transcriptome, which could be attributed to the time passed from seeding (Figure S2B) or the population doubling (Table S2). After undergoing heat shock, the proportion of DEGs that were downregulated (54%) was nearly equal to the proportion of upregulated DEGs (46%) (Figure S2C). Several genes were also evaluated by RT-qPCR to support the sequencing results (Figure S3).

We found that the various HS treatments significantly changed the expression levels of a total of 3667 genes (padj $\leq$0.05 and log2(FC)$\geq$1) (Figure 1C). After a 6-h HS, 712 differentially expressed genes

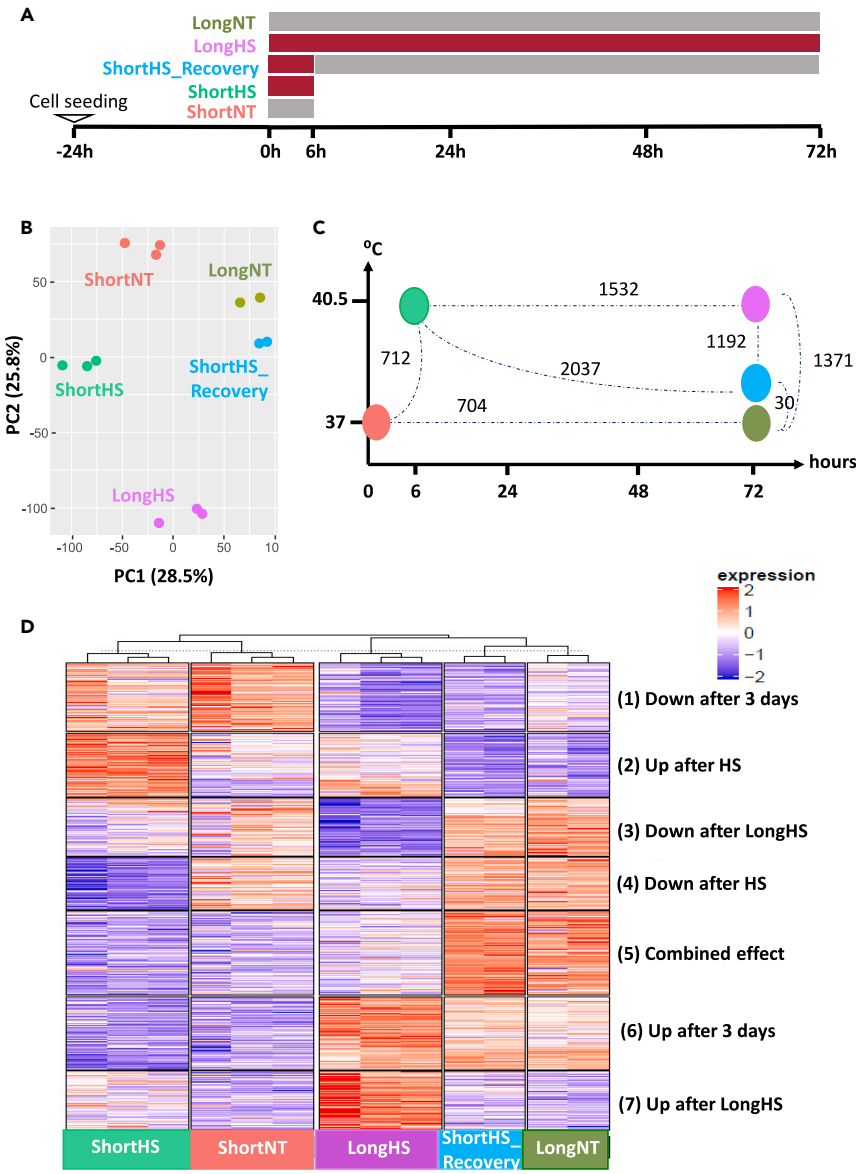

Figure 1. Transcriptome changes in response to heat shock

Related to Figures S1–S3.

(A) A schematic timeline showing the HS treatments from which RNA-Seq libraries were prepared. MSCs were plated and 24 h later exposed to heat shock (HS, 40.5°C) for: 6 h (ShortHS), 6 h + 3 days recovery at 37°C (ShortHS_Recovery), 72 h (LongHS), followed by collection for RNA extraction. Control cells were parallelly plated and maintained in normal temperature (NT, 37°C). Each treatment has color code, which is be used throughout the article: **ShortNT (red), ShortHS (green), LongNT (olive), ShortHS_Recovery (blue), LongHS (purple)**.

(B) Scatterplot for principal component analysis of global gene expression (RNA-seq) demonstrates clear separation of gene transcripts between groups.

(C) Number of differentially expressed genes (DEGs) with padj $\leq$0.05 and log2(FC)$\geq$1 that change between the treatment groups.

(D) Heatmap of K-means clustering results in 3667 DEGs between the treatment groups. Expression in blue indicates downregulation and red indicates upregulation.

(DEGs) were found, whereas after a three-day HS 1,371 DEGs were found, most downregulated (Figure S2C). In the cells that were allowed to recover at 37°C for three days after the short HS, 2,037 genes were changed versus the short HS. However, only a slight difference is found when compared to the long NT sample. This suggests that after a short HS, there is a major recovery from the stress, at least on

the transcriptional level. The results indicate that short thermal shock affects MSCs' gene expression rapidly and widely but mostly transiently.

To discern the dominant systematic changes following the different HS treatments, we performed k-means clustering on all 3,667 DEGs (Figure 1D). The resulting clusters revealed three major modes of change. Clusters 2 and 4 show the common effect of both long and short HS on the transcriptional pattern. Conversely, in clusters 3 and 7, the change is only observed after the long HS, portraying that more genes were induced after three days, possibly due to a slower transcriptional response rate. Finally, clusters 1 and 6 show the effect of culturing time on the transcriptional pattern.

While changes in expression patterns are evident from the k-means clustering analysis, we wanted to systematically examine the transcriptional changes following each treatment alone and identify specific biological features and processes.

Cell cycle and immune response are downregulated as developmental pathways are activated following a long heat shock

To get a comprehensive understanding of all the changes that occurred following the HS, we delved into the analysis of each treatment using the gene set enrichment analysis (GSEA) and gene ontology (GO) tools (as described in the bioinformatic analysis supplementary). First, we focused on the changes observed in cells exposed to long HS vs. long NT control (Figure 2A). On the morphological level, cells appeared flattened, with expanded cytoplasm and detectable nuclear stress granules-like formation (Figures 2B and S4A).[37] On the transcriptional level, 1,371 DEGs (padj $\leq$0.05 & log2(FC)$\geq$1) were found (Figure 1C). GSEA analysis shows downregulation of cell proliferation and metabolism, namely hallmarks for cell cycle and DNA repair, glycolysis and oxidative phosphorylation (see Figures S4B and S4C for a more detailed view and experimental support of cell cycle related genes expression) and upregulated response to stress (Figure 2C, all hallmarks with normalized enrichment above 1). There is also downregulation of gene sets related to inflammation and the immune system, as well as DNA damage and ROS response (Figure 2C upper lines). This could be explained by the long duration of the HS, which might have required the cells to attenuate their stress response. Interestingly, many genes related to differentiation and cell-fate related pathways (Figures 2C and 2D) were also upregulated, as previously suggested.[38] For example, general terms of cell growth and morphogenesis were enriched, as well as more specific terms like connective tissue, chondrocytes, osteoblasts, kidney, and neuronal system were upregulated (Figure 2D). We confirmed this effect in tissue culture by utilizing a widely used chondrogenesis differentiation protocol on the MSCs after the HS treatments (as in.[15] Our findings indicated that, as anticipated from the alteration in gene expression, the Long_HS treatment significantly enhanced the efficiency of chondrogenesis (Figure S4D). In addition, there is apparent upregulation of cell adhesion molecules (Figure S4E), which represents cell-cell interactions and the interaction between the cell and the extracellular matrix (ECM).[39] These molecules promote a broad spectrum of cell signaling that directly or indirectly modulates stem cell proliferation, self-renewal property, adhesion, and multilineage differentiation.[39,40] Accordingly, KEGG analysis showed enrichment and upregulation of pathways such as MAPK, PI3K-Akt, RAS and RAP1 (Figure 2E). In general, those pathways are known to regulate cell size, survival, differentiation, adaptation to growth conditions, and stress responses.[41] PI3K-Akt activates the mTOR signaling pathway,[41,42] which is also elevated following HS in bovine granulosa cells.[38] Activation of PI3K-Akt and mTOR pathways plays a central role in cellular senescence and organismal aging and thus acts as a driver of stem cell depletion and reduced tissue regenerative capacity.[43–45] What is more, these changes were accompanied by the upregulation of post-translational modifiers, specifically histone demethylases and Polycomb group (PcG) complex members (Figure 2F), which probably regulate the observed transcriptional changes.

In summary, our data demonstrate that three days of HS treatment are not detrimental to cell viability but have a major effect on cell fate and aging. Although the impact of long HS on differentiation might prove useful as a pretreatment protocol for MSC transplantations, this duration of HS is scarcely experienced in physiological settings. Hence, we wished to examine the effect of short (6 h) HS on the MSCs.

Stress responses are induced while cellular functions decline following a short heat shock

We focused on the immediate effects of short HS (Figure 3A) using all available tools for enrichment analysis.[46] First, GSEA analysis of all genes showed that five out of the ten most upregulated genes in this treatment (HSPA1A, HSPA6, HSPA4L, HSPB1, HSPH1; see Figure 3B, red arrow) were HS genes, along with

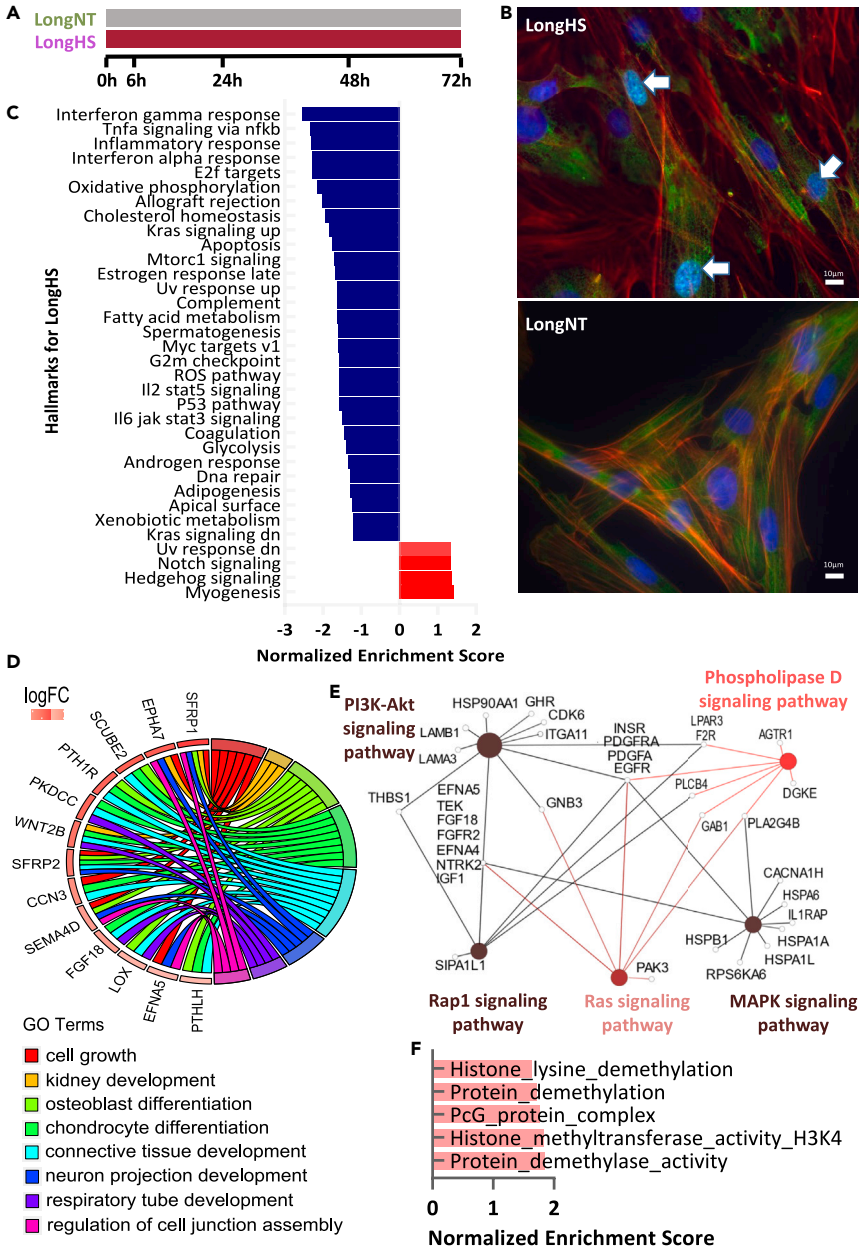

Figure 2. Downregulation of cell cycle and immune response genes while developmental pathways genes are induced following long heat shock

Related to Figure S4.

(A) Illustration of long heat shock treatment.

(B) Cells after LongHS stained with G3BP1 (green), actin filaments stained with phalloidin (red) and nuclei stained with DAPI (blue). Imaging was done using Nikon ECLIPSE TI-DH Florescent Microscope, scale bar = 10 μm. Turquoise nuclei marked with arrows contain the stress granules. No stress granules were found in LongNT.

(C and D) (C) Results of Gene set enrichment analysis (GSEA) Hallmark analysis showing significantly enriched gene sets (FDR q < 25% and p < 0.05). A positive normalized enrichment score value, in red, indicates enrichment in the LongHS phenotype (upregulated gene sets in LongHS). Negative enrichment, in blue, indicate enrichment in the LongNT phenotype (downregulated in LongHS). Upregulated heat stress genes and redox maintenance related genes are marked by red and green errors, respectively, while downregulated genes are pointed at by blue errors (D) Differentiation pathways significantly (padj < 0.05) upregulated in LongHS vs. LongNT as per g:Profiler GO analysis, and their associated genes are presented in GOChord plot. The plot's left half shows the DEGs shared by at least 3 differentiation pathways

Figure 2. *Continued*
and the right half displays the GO terms related to differentiation pathways marked in various colors. The colored bands connect a gene to a specific GO term. The scale bar presents gene's log2FC.
(E) KEGG pathways significantly enriched in upregulated DEGs of LongHS vs. LongNT presented by ClueGo pathway analysis and visualization. Colors represented p value: light red 0.05, red 0.01, brown 0.001. The node size represents the term enrichment significance.
(F) Significantly enriched (FDR q < 25% and p < 0.05) upregulated GSEA GO terms related to histone modifications and PcG complex following LongHS.

genes that regulate redox maintenance (SLC27A5), insulin levels (MAFA) and mitotic progression (MISP) (Figure 3B, marked with green arrow). The most downregulated genes following short HS (blue arrow) are involved in RNA interference (RNAi) process (TSNAX), post-splicing multiprotein complex (UPF3A), cell polarity (DAAM2), metabolism regulation (DHRSI2) and chromatin and transcription process (H1-2). Second, these genes are mostly included in the Hallmark gene sets enriched for up- and down-regulated processes following 6 h HS (Figure 3C). Short HS induced stress response and differentiation pathways while halting oxidative phosphorylation and cell cycle. Third, upregulated biological processes enriched in GSEA were stress response, autophagy, development, and mRNA transcription, while downregulated processes were all related to DNA replication (Figure 3D, Table S3). Fourth, in addition to GSEA, we analyzed the DEGs using g:Profiler (GO, KEGG, and Reactome) and found enrichment of DNA replication, with an emphasis on initiation in the downregulated DEGs (Figure 3E), whereas stress response and ER activity were enriched in the upregulated DEGs (Figure 3F). After discovering dramatic short-term changes, we checked how many of these changes remained stable. To elucidate these stable changes, the treated cells were allowed to recover in normothermia for three days before the transcriptional analysis.

Long term effects of short heat stress

To identify the transcriptional changes which occurred after short HS but remained stable even after three days of recovery, we examined the three different time points: control (as the zero-time point), 6 h HS and 6 h HS followed by three day recovery (ShortNT vs. ShortHS vs. ShortHS_Recovery, Figure 4A). Thus, we re-analyzed the data, focusing our attention on the transcriptional pattern of all DEGs between ShortNT and ShortHS (see supplementary methods) and used K-means clustering to visualize the patterns of the transcriptomic differences (Figure S5A). To further confirm the validity of our results, we removed all DEGs related to the time in culture (Short_NT vs. Long_NT) from the list of DEGs. We re-performed the K means analysis (Figure 4B, see STAR methods for details). Instead of 4521 DEGs with culturing effect, we were left with 3993 DEGs without culturing effect. While after recovery, most genes regained similar expression levels to that of the control sample (Figure 4B clusters 1 and 4), two clusters in which the differential expression persisted were identified. Cluster 2 genes were lowly expressed in the control sample but were upregulated after the short HS and remained active after recovery. g:Profiler analysis (GO, KEGG and Reactome) resulted in enriched biological processes related to stress and protein degradation in this cluster (Figures 4C and S5B). This implies that some elements of the stress response to acute stress last for more than three days. Cluster 3 is the mirror image of Cluster 2, presenting stably downregulated genes related to proliferation and metabolism but also senescence and DNA damage (Figure 4D and Cluster 7 in Figure S5C). This might suggest that following short HS, the cells enter a state of quiescence to maintain their stemness. These data are in agreement with our population doubling time analysis, which shows slower proliferation after both the long and the short HS (Figure 4E).

A similar analysis done on the other two clusters, 1 and 4, raised an interesting point. Of the most 25 significantly enriched GO terms in cluster 4, only 3 are unrelated to transcriptional regulation, mostly epigenetic modification (Figures 4F and S5D). This raised the intriguing hypothesis that the epigenetic landscape is altered following the short HS, possibly with long term consequences. To examine how a short period of stress could have that kind of persistent effect, we used the EpiFactors Database[47] and related MGI[48] annotations to identify enriched epigenetic modifiers in the data. Several epigenetic complexes were found highly enriched in Cluster 4, i.e., upregulated after 6 h HS and then back to low expression after recovery (Figure 4G). Interestingly, those complexes are all related to the mixed lineage leukemia (MLL) proteins which catalyze the trimethylation of histone H3 Lys 4 (H3K4me3), a mark associated with active or poised transcription and found in the promoters of most active or poised genes.[49] Bivalent genes are lineage-specification genes that carry both H3K4me3 and H3K27me3 histone marks and are regulated by the balance between the two histone marks. This balance is mediated by PcG members and the MLL coactivator complex.[50] We searched for known targets of the MLL complex in our list. We found cluster 2 (i.e.,

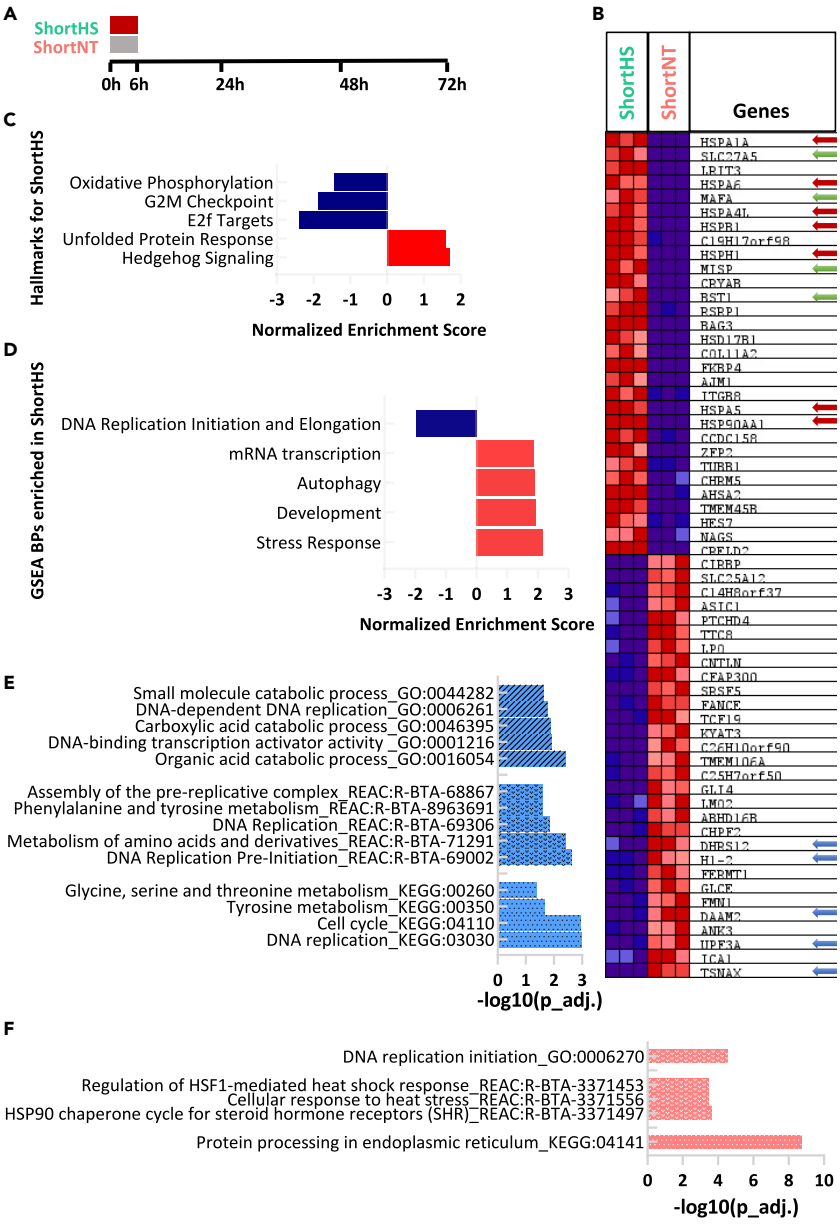

Figure 3. Induced stress response and reduced cellular functions following short heat shock

(A) Illustration of short heat shock treatment.

(B) Heatmap of the top 30 marker genes for each phenotype in the comparison of ShortHS (left columns) vs. ShortNT (right columns). Expression values are represented as colors and range from red (high expression) to dark blue (lowest expression).

(C) Results of GSEA Hallmark analysis showing enriched gene sets (FDR q < 25% and p < 0.05). A positive normalized enrichment score values, marked in red, indicate enrichment of upregulated hallmarks in the ShortHS phenotype, while negative enrichment, marked in blue, indicate enrichment in ShortNT. green, red, and blue arrows indicate.

(D) Results of GSEA biological processes significantly enriched (FDR q < 0.25 and p < 0.01) in the comparison of ShortHS vs. ShortNT. Due to high number of GOs, the GOs with similar process were combined under one general phrase (Table S3). A positive normalized enrichment score is the average of combined terms.

(E and F) (E) Significantly (padj < 0.05) enriched GO terms, KEGG and Reactome pathways in downregulated and (F) upregulated DEGs in ShortHS vs. ShortNT cells using g:Profiler.

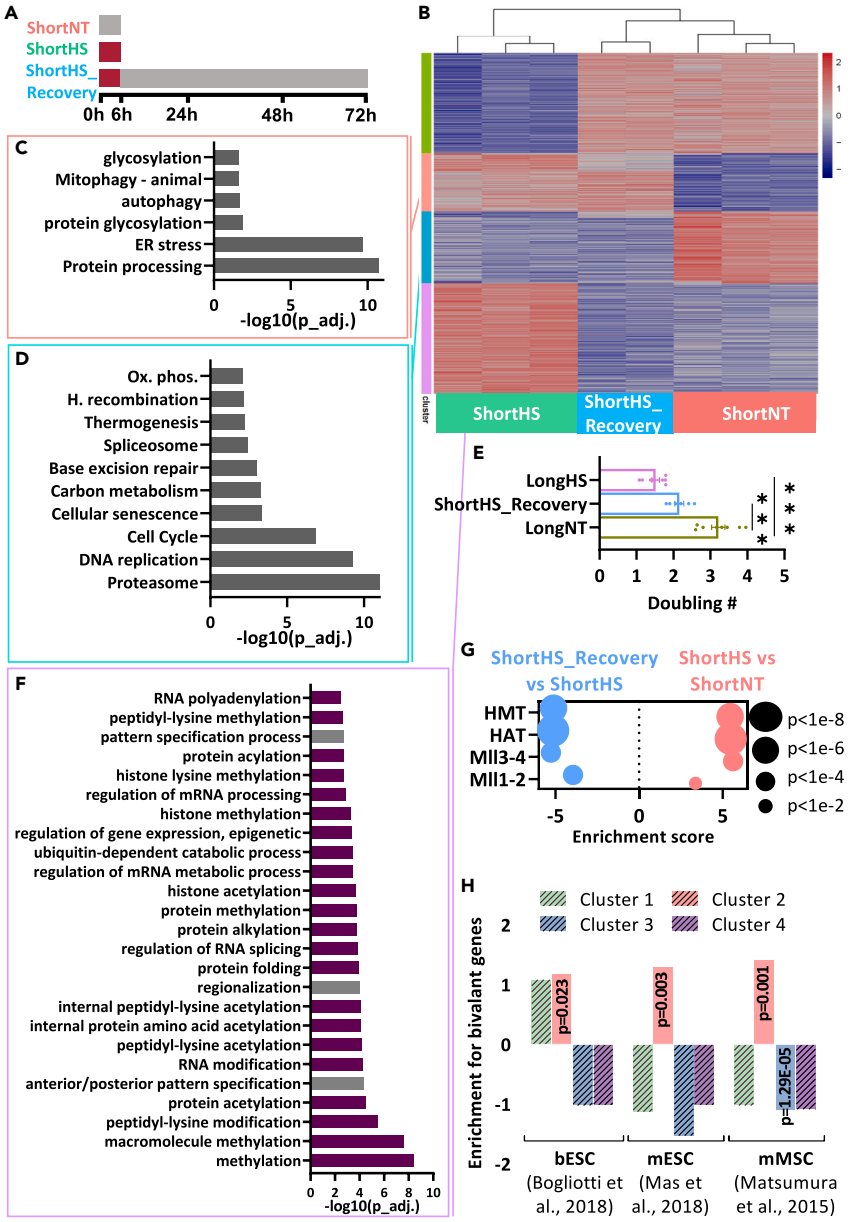

Figure 4. Transient upregulation of chromatin modifiers after short heat shock and stable activation of lineage commitment genes, maintained after three day recovery

Related to Figures S5 and S6.

(A) Illustration of ShortHS_Recovery vs. ShortHS treatment.

(B) Heatmap of K-means clustering results for differentially expressed genes (padj <0.05) between ShortHS and ShortNT.

(C) Enrichment of biological processes from g:Profiler enriched in cluster 2.

(D) Enrichment of biological processes from g:Profiler in cluster 3.

(E) Population doubling time for prolonged treated groups. Data are the mean ± s.e.m. (n = 6). All p values were calculated using Kruskal-Wallis non parametric test, ***p < 0.001.

(F) Enrichment of biological processes from g:Profiler in cluster 4.

(G) Hypergeometric enrichment analysis of MLL (GO:0044665, GO:0044666), HAT (GO:0000123) and HMT (GO:0035097) complexes showing upregulated complexes following ShortHS that return to normal or downregulated during recovery period. The node size represents the p value.

(H) Hypergeometric enrichment analysis of bivalent genes, showing bivalent genes upregulation following ShortHS that remain in this state even after recovery period.

upregulated in both short- and long-term) to be significantly enriched for bivalent genes[51–53] in contrast to the other clusters, where these and other bivalent genes were significantly underrepresented (Figure 4H). The full list of DEGs is similarly enriched (Figure S5E). Those bivalent DEGs are crucial to cell fate regulation: several FGF family members, FZD3, JUN, FOXF1, VEGFA, and KDM6B, to state a few (Figure S6). Overall, these data shed light on the long-term effects of short HS and suggests that a short stress event can modulate the epigenetic regulation of key cell fate genes.

Next, we wished to uncover the transcriptional changes shared by all HS-treated cells.

Key characteristics of MSC vary with heat stress duration

So far, we have shown considerable effects of short and long HS *in vitro*. To examine to what extent the DEGs are shared between the time points, we had to eliminate the effect of culturing time and the circadian clock and focus solely on the effect of HS. To that end, we removed all DEGs that changed between the short and long NT controls (see supplementary methods for the analysis) and examined which DEGs were commonly upregulated (Figure 5A) or downregulated (Figure 5B) in all HS. A total of 102 upregulated and 93 downregulated DEGs were shared by short and long HS treatments, a highly significant enrichment over what could be expected by chance. While g:Profiler analysis showed that the commonly upregulated genes were related to stress response, the commonly downregulated genes were not significantly enriched to any specific pathway or process. Hence, we looked for common GSEA hallmarks, which were enriched after both short and long HS. Interestingly, important cellular functions like oxidative phosphorylation and cell cycle were found to be impaired in all HS; the immune system was downregulated, and the hedgehog signaling pathway was significantly upregulated following HS, even after the recovery period (Figures 5C, S7A, S7B, S8A, and S8B).

To understand the effect of HS on the biological processes related to the key capacities of MSCs, namely self-renewal, differentiation and immunomodulation, we compared the relevant biological processes and functions between different treatments. Zooming in on cell cycle related annotations, we saw that while in all three treatments the downregulated DEGs were enriched for the general term 'cell cycle', only the short HS is downregulating specifically DNA replication pre-initiation (e.g., genes like MCM2 and 7, CDC6 and E2F1). Furthermore, the LongHS and ShortHS_Recovery samples showed downregulation of genes required for the G2/M phase (namely cyclin A and B and CDC25), suggesting a block before mitosis (Figure 5D). Remarkably, the cells that got the short HS but were left to recover for three days in normothermia show both the G1/S and the G2/M effects, although to a lesser degree, suggesting that even short thermal stress might disrupt cell cycle regulation and proliferation. These results are supported by the population doubling we saw in the culture following the experiments (Figure 4E) as well as in our previously described cell cycle analysis.[15]

As for differentiation, it appears that several developmental pathways were activated depending on the heat shock treatment (Figures 5E, S9A, and S9B). The long HS induced various differentiation pathways; the most enriched were the differentiation to mesoderm/mesenchymal fate. Notably, both canonical and non-canonical WNT pathways were upregulated after long HS, suggesting a general shift in cell identity. The short HS upregulates the canonical WNT but downregulates the non-canonical (WNT5a related) pathway (Figures 5E, S9A, and S9B). In line with the fact that KEGG definitions like "canonical WNT pathway" includes both activators and suppressors, this and other pathways are enriched in both the down and upregulated DEGs. Interestingly, HOX genes related to skeletal morphogenesis and several epigenetic factors (e.g., Setd2, Kdm6a, Jarid1) were upregulated following both long and short HS, suggesting that heat shock treatment may slow proliferation while promoting MSC's commitment and differentiation.

Immunomodulatory properties of MSCs have previously been shown to decline following stress.[15,54] Major downregulation of immune related pathways was detected after HS (Figure 5F). GO analysis in GSEA revealed considerable effects on the production of interleukins (ILs), TNFs and INF-ɤ. In addition, we observed the downregulation of antigen processing, acute inflammatory response, response to chemokines, and the migration and chemotaxis of macrophages, neutrophils, and granulocytes (Table S4). List of 760 genes in the "Cytokine Signaling in Immune system SuperPath" (https://pathcards.genecards.org) was analyzed and 38 of them (for example IL1Rs, IL7 and IL18) were downregulated after long HS while 17 (like FGF2 and FGFR2 which are related to differentiation[55,56]), are upregulated (for detailed list of genes see Table S5). Overall, genes related to IL production are significantly downregulated (hypergeometric p = 2.49e-04, Figure 5G).

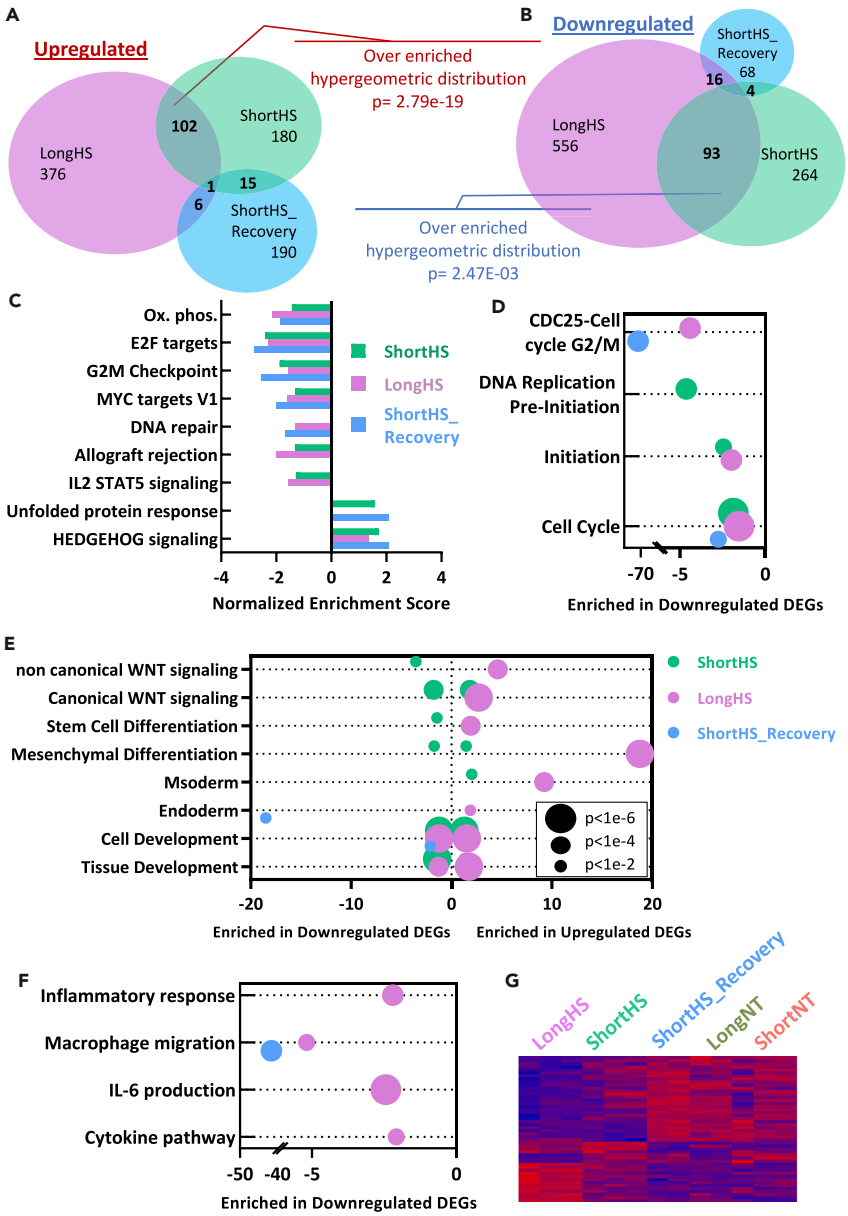

Figure 5. Cell cycle and metabolism are commonly reduced following all heat shock protocols, while other processes related to key characteristics of MSC are differently regulated

Related to Figures S7–S9.

(A) Venn diagram of upregulated genes (padj <0.05) between the treatment groups.

(B) Venn diagram of downregulated genes (padj <0.05) between the treatment groups.

(C) Heat shock common GSEA hallmark gene sets (FDR q < 25% and p < 0.05) and their enrichment score.

(D) Hypergeometric enrichment analysis of cell cycle related biological processes, effected by HS, and their enrichment score. N00455: CDC25-Cell cycle G2/M (KEGG pathway), GO:0007049: Cell cycle (MGI database), R-BTA-69002 – DNA Replication Pre-Initiation (Reactome). Size node represents p value as indicated in E.

(E) Hypergeometric enrichment analysis of biological processes related to development effected by HS. GO:0060070: Canonical WNT signaling, GO 0048863: Stem cell differentiation, GO:0048468: Cell development, GO:0009888: Tissue development, GO:0007492: Endoderm development. GO:0007498: Mesoderm development, GO:0048762: mesenchymal cell differentiation. The legends in this graph – enriched groups and p values - are applicable also to D and F.

(F) Hypergeometric analysis of biological processes related to immune system effected by HS. GO:0002526: Acute Inflammatory response, GO:1905517: Macrophage migration, GO:0032635: IL-6 production, Cytokine pathway list was taken from PathCards v5.7.551.0. Size node represents p value as indicated in E.

(G) Heatmap of cytokine pathways genes that are differentially expressed in LongHS vs. LongNT.

DISCUSSION

Here, we show that the transcriptional changes following heat shock *in vitro* are broad and can alter every functional aspect of MSC identity. We analyzed RNA-seq from bUC-MSCs in normothermia vs. short or long exposures to HS, to investigate the subsequent changes in the transcriptional landscape that might lead to a shift in the cell's identity and fate. We were particularly interested in identifying the long-term effect of thermal stress on cell proliferation, differentiation, and immunomodulation capacities; as those key MSC features were amongst the most abundant GO term groups. To examine the relevance of our data to physiological HS, we compared our DEGs to a list of 55 genes defined as thermal stress responsive in a bovine study done *in vivo*[57]: 36 of the 55 genes were found to be differentially expressed following short, long or both HS groups. The genes EIF2A, HSPA1A, HSP90AA1, and HSF1 were considered by the authors as key genes that responded to thermal stress of Holstein dairy cattle. From our experiments, HSPA1A and HSP90AA1 were indeed upregulated DEGs for short and long HS groups, and EIF2A for shortHS group only. HSF1 was not differentially expressed in our treatments, maybe due to our use of 40.5°C which is mild relative to the 42°C used by the authors. In addition, the bioinformatic analyses of Fang et al. (2021[57]) pinpointed biological processes and pathways associated with thermal stress that are very similar to those identified, e.g., protein folding, transcription factor binding, immune effector process, negative regulation of cell proliferation, PI3K- Akt signaling pathway, and MAPK signaling pathway.

The immediate transcriptional changes found following short HS include the onset of several cellular stress responses and cell-cycle arrest in G1/S. This checkpoint arrest is a known adaptive cellular response to HS, in which cells slow proliferation rate while rapidly upregulating transcription and translation of HSPs to maintain cell homeostasis and retain their cellular functions.[2] Our previous results, which showed cell-cycle arrest at G1/S after short HS[15] also support this finding. Two possible interpretations arise, each with a different implication for stemness and differentiation: in one, following the short HS the cells enter a quiescent state; this is in alignment with the observed metabolic changes (reduced amino acid metabolism, reduced oxidative phosphorylation, increased glycolysis, and mitophagy induction of mitochondrial renewal, etc.), as reviewed in.[58] This suggests that short HS treatment encourages the retention of MSC stemness. In the other interpretation, a long G1 may allow for the accumulation of the epigenetic changes needed for the initiation of fate decisions.[59] This interpretation might explain the transient upregulation of many epigenetic factors and the stable changes in many lineage commitment genes observed after three day recovery. To mechanistically challenge those two interpretations and to determine whether HS promotes stemness or differentiation, further study, preferably on the single cell level, is required to mechanistically challenge these two interpretations.

Evident changes were observed in the morphology and proliferation rate of the cells three days after the Short or Long HS treatment. However, on the transcriptional level, the majority of ShortHS DEGs reverted to normal expression levels after three days recovery, and only a subset of the DEGs remained. In this subset of stable DEGs we see the upregulation of several developmental genes known as "bivalent" for their dual histone lysine tri-methylation marking in both K4 (active mark) and K27 (repressive mark). Those genes are known targets of the MLL complex, which carries out the methylation of histone H3 lysine 4 and was transiently overexpressed after the initial HS event. So, a sequence of events can be hypothesized. First, the short HS upregulates the MLL complex members, thus shifting the balance between the active and repressive histone marks. Consequently, the chromatin of the previously poised (and silent) bivalent genes opens to enable transcription of developmental genes, priming the cells toward cell fate determination. Evaluation of this hypothesis will require follow-up studies examining changes in epigenetic marking following HS.

The idea that cells after HS pretreatment are more prone to differentiation is tempting. If indeed priming MSCs by specific stress can help us direct their fate, it could provide us with another tool in the cellular therapy toolbox. Moreover, as the idea of cellular agriculture, or cultured meat, gains increasing attention, more cost effective and clean ways to differentiate the source cells toward the intended fate (usually muscle or fat) are needed. Current differentiation protocols require large amounts of expensive and unstable growth factors, which raise costs and hinder commercialization of cultured meat. Every pretreatment protocol that is easy, cheap, and reduces the time and resources necessary for differentiation will have huge economic and environmental consequences.

On the clinical level, it is interesting to note the negative effect of long HS on MSC immune activity, possibly compromising the cells' immunomodulatory functions. Indeed, reduced immunomodulation was

previously observed when we co-cultured MSCs subjected to HS with macrophages.[15] The reduced immunomodulation capacity of the stressed MSCs might account for the increased production of inflammatory cytokines found in mammary epithelial cells following HS.[60] Hence, the increased rates of inflammatory diseases in dairy cows during the summer months could be partially attributed to the failure of the malfunctioning MSCs to modulate the inflammatory response of the surrounding cells to HS. Overall, identifying the long-term effect of HS on MSC capacities suggest an explanation for the seeming contradiction between the *in vitro* experiments which show beneficial effects to HS priming and the *in vivo* data that demonstrate harmful physiological consequences to thermal stress (reviewed by[61]).

Although we have demonstrated that HS affects MSCs' transcriptome, our study has some limitations. Population heterogeneity, circadian clock, culturing time, and culture conditions all have effects on RNA-seq results that need to be controlled for (Figure S10). To counter this drawback, we (1) made sure that at the end of the experiment (either 6 h or 3 days) all the treatment groups had similar culture density (Table S2), (2) sequenced two or three independent biological repeats from each treatment group (Table S1), and (3) reduced heterogeneity that might originate in genetic background, by using the same MSC line in all three repeats. To counter the effects of culturing time, we used untreated (NT) controls, one for the short HS, and the other for the long HS. When we compared gene expression at the short and long time points, all DEGs that were apparent between the NT control time points (and were assumed to be the result of culturing effect) were ignored. Interestingly, two transcription factors regulating the circadian clock, BHLHE40 and TIMELESS, were found among those ignored DEGs. These two transcription factors together regulate the expression of 202 other DEGs in this group (Figure S10B). These oscillating genes may partly explain the relatively high number of DEGs due to culturing effect since the ShortHS and ShortNT samples were taken at noon (24 h after seeding + 6 h treatment) while the three-day samples (LongHS, LongNT and ShortHS_Recovery) were collected in the morning (exactly 96 h after seeding).

One very obvious limitation of this study is its restriction to *in vitro* cell experiments. Also, there is lack of whole transcriptome data, presence of which could have strengthened the role of molecular players of this study in breast cancer progression. Another limitation is that this study only focused on two VEGFA transcripts, whereas further research could explore the expression patterns and alternative splicing of other VEGFA transcripts under hypoxic condition. Future research must also elucidate the detailed mechanism behind SRSF2 regulating methylation status on VEGFA via DNMT3A. Moreover, it is important to note that *miR-222-3p* has multiple targets other than SRSF2, which could potentially play a role in regulating other cancer-related processes. This avenue of research warrants further exploration.

Conclusions

The use of MSCs for cell therapy or cultured meat has several advantages, such as high availability, low production price, and fast and easy differentiation. Nonetheless, our limited understanding of their heterogeneity, fate determination, and immunomodulation holds back further MSC applications. It is therefore essential to improve the consistency and efficacy of MSCs. Such enhancement can be achieved using *in vitro* preconditioning treatments such as HS.[62] Here we show that the correct application of HS allows for the enhancement of desired MSC characteristics and induction of a wide range of stem cell fates and differentiation pathways.

Limitations of the study

Specific conditions were carefully chosen for the HS treatments in this study. However, it is important to acknowledge that there are many other time points and durations of HS treatments that warrant further investigation. Additionally, the impact of cold shock was not examined in this particular study. Furthermore, incorporating additional repeats from different lines of MSCs derived from a broader range of animals and cow breeds would improve the statistical significance of our findings. The study primarily focused on analyzing transcriptional changes and inferring their influence on epigenetic modifications. Future studies should consider mapping the epigenetic changes following HS using alternative methodologies.

STAR★METHODS

Detailed methods are provided in the online version of this paper and include the following:

- KEY RESOURCES TABLE

SUPPLEMENTAL INFORMATION

Supplemental information can be found online at https://doi.org/10.1016/j.isci.2023.107305.

ACKNOWLEDGMENTS

This work was funded by a US-Israel Binational Agricultural Research and Development Fund research project #IS-5067-18, The Israeli Dairy Board grant # 820-0341 and the Israeli Ministry of Agriculture and Rural Development grant #12- 04-0014. We are grateful to all the members of the Schlesinger lab for their ideas and support; Dr. Asaf Marco for help with the bioinformatic analysis, Prof. Z. Roth for scientific discussion, encouragement and support; Joseph Kippen for critical reading and reviewing; the Weizmann Institute Next Generation Sequencing Facility, for sequencing support; The authors also thank Dr. S. Shainin and Mr. S. Yaakobi from the Volcani Center for help with obtaining the umbilical cords. Graphical abstract was Created with BioRender.com.

AUTHOR CONTRIBUTIONS

I.R.H.: conception and design, designing and performed the experiments, bioinformatics analysis and data interpretation, and manuscript writing. G.S.: validation of MSC lines by flow and RT-qPCR. C.S.: support with MSC extraction and culturing. S.S.: conception and design, assembly of data and data analysis, manuscript writing. The authors read and approved the final manuscript.

DECLARATION OF INTERESTS

The authors declare that they have no competing interests.

INCLUSION AND DIVERSITY

We support inclusive, diverse, and equitable conduct of research.

Received: December 22, 2022
Revised: May 23, 2023
Accepted: July 3, 2023
Published: July 10, 2023

REFERENCES

1. Peters, A., Nawrot, T.S., and Baccarelli, A.A. (2021). Hallmarks of environmental insults. Cell *184*, 1455–1468. https://doi.org/10.1016/J.CELL.2021.01.043.

2. Richter, K., Haslbeck, M., and Buchner, J. (2010). The Heat Shock Response: Life on the Verge of Death. Mol. Cell *40*, 253–266. https://doi.org/10.1016/J.MOLCEL.2010.10.006.

3. Kitagawa, Y., Suzuki, K., Yoneda, A., and Watanabe, T. (2004). Effects of oxygen concentration and antioxidants on the in vitro developmental ability, production of reactive oxygen species (ROS), and DNA fragmentation in porcine embryos. Theriogenology *62*, 1186–1197. https://doi.org/10.1016/J.THERIOGENOLOGY.2004.01.011.

4. Agarwal, A., Virk, G., Ong, C., and du Plessis, S.S. (2014). Effect of Oxidative Stress on Male Reproduction. World J. Mens Health *32*,

1–17. https://doi.org/10.5534/WJMH.2014.32.1.1.

5. de Barros, F.R.O., and Paula-Lopes, F.F. (2018). Cellular and epigenetic changes induced by heat stress in bovine preimplantation embryos. Mol. Reprod. Dev. *85*, 810–820. https://doi.org/10.1002/MRD.23040.

6. Olde Riekerink, R.G.M., Barkema, H.W., and Stryhn, H. (2007). The Effect of Season on Somatic Cell Count and the Incidence of Clinical Mastitis. J. Dairy Sci. *90*, 1704–1715. https://doi.org/10.3168/JDS.2006-567.

7. Chen, S., Wang, J., Peng, D., Li, G., Chen, J., and Gu, X. (2018). Exposure to heat-stress environment affects the physiology, circulation levels of cytokines, and microbiome in dairy cows. Sci. Rep. *8*, 14606. https://doi.org/10.1038/s41598-018-32886-1.

8. Key, N., Sneeringer, S., and Marquardt, D. (2014). Climate Change, Heat Stress, and U.S. Dairy Production. SSRN J. https://doi.org/10.2139/ssrn.2506668.

9. Dado-Senn, B., Laporta, J., and Dahl, G.E. (2020). Carry over effects of late-gestational heat stress on dairy cattle progeny. Theriogenology *154*, 17–23. https://doi.org/10.1016/J.THERIOGENOLOGY.2020.05.012.

10. Roth, Z. (2017). Effect of Heat Stress on Reproduction in Dairy Cows: Insights into the Cellular and Molecular Responses of the Oocyte. Annu. Rev. Anim. Biosci. *5*, 151–170. https://doi.org/10.1146/annurev-animal-022516-022849.

11. Kawano, K., Sakaguchi, K., Madalitso, C., Ninpetch, N., Kobayashi, S., Furukawa, E., Yanagawa, Y., and Katagiri, S. (2022). Effect of heat exposure on the growth and developmental competence of bovine oocytes derived from early antral follicles. Sci. Rep. *12*, 8857. https://doi.org/10.1038/s41598-022-12785-2.

12. Sharma, S., and Bhonde, R. (2020). Genetic and epigenetic stability of stem cells: Epigenetic modifiers modulate the fate of mesenchymal stem cells. Genomics *112*, 3615–3623. https://doi.org/10.1016/J.YGENO.2020.04.022.

13. Xue, Y., and Acar, M. (2018). Mechanisms for the epigenetic inheritance of stress response in single cells. Curr. Genet. *64*, 1221–1228. https://doi.org/10.1007/S00294-018-0849-1.

14. Chen, X., Wang, Q., Li, X., Wang, Q., Xie, J., and Fu, X. (2018). Heat shock pretreatment of mesenchymal stem cells for inhibiting the apoptosis of ovarian granulosa cells enhanced the repair effect on chemotherapy-induced premature ovarian failure. Stem Cell Res. Ther. *9*, 240. https://doi.org/10.1186/S13287-018-0964-4.

15. Shimoni, C., Goldstein, M., Ribarski-Chorev, I., Schauten, I., Nir, D., Strauss, C., and Schlesinger, S. (2020). Heat Shock Alters Mesenchymal Stem Cell Identity and Induces Premature Senescence. Front. Cell Dev. Biol. *8*, 565970. https://doi.org/10.3389/fcell.2020.565970.

16. Garner, J.B., Chamberlain, A.J., Vander Jagt, C., Nguyen, T.T.T., Mason, B.A., Marett, L.C., Leury, B.J., Wales, W.J., and Hayes, B.J. (2020). Gene expression of the heat stress response in bovine peripheral white blood cells and milk somatic cells in vivo. Sci. Rep. *10*, 19181. https://doi.org/10.1038/s41598-020-75438-2.

17. Yue, S., Wang, Z., Wang, L., Peng, Q., and Xue, B. (2020). Transcriptome Functional Analysis of Mammary Gland of Cows in Heat Stress and Thermoneutral Condition. Animals. *10*, 1015. https://doi.org/10.3390/ANI10061015.

18. Collier, R.J., Stiening, C.M., Pollard, B.C., VanBaale, M.J., Baumgard, L.H., Gentry, P.C., and Coussens, P.M. (2006). Use of gene expression microarrays for evaluating environmental stress tolerance at the cellular level in cattle. J. Anim. Sci. *84*, E1–E13. https://doi.org/10.2527/2006.8413_SUPPLE1X.

19. Sammad, A., Luo, H., Hu, L., Zhu, H., and Wang, Y. (2022). Transcriptome Reveals Granulosa Cells Coping through Redox, Inflammatory and Metabolic Mechanisms under Acute Heat Stress. Cells *11*, 1443. https://doi.org/10.3390/CELLS11091443.

20. Dou, J., Cánovas, A., Brito, L.F., Yu, Y., Schenkel, F.S., and Wang, Y. (2021). Comprehensive RNA-Seq Profiling Reveals Temporal and Tissue-Specific Changes in Gene Expression in Sprague–Dawley Rats as Response to Heat Stress Challenges. Front. Genet. *12*, 420. https://doi.org/10.3389/FGENE.2021.651979.

21. Schultz, M.B., and Sinclair, D.A. (2016). When stem cells grow old: phenotypes and mechanisms of stem cell aging. Development *143*, 3–14. https://doi.org/10.1242/DEV.130633.

22. Ermolaeva, M., Neri, F., Ori, A., and Rudolph, K.L. (2018). Cellular and epigenetic drivers of stem cell ageing. Nat. Rev. Mol. Cell Biol. *19*, 594–610. https://doi.org/10.1038/s41580-018-0020-3.

23. Pittenger, M.F., Mackay, A.M., Beck, S.C., Jaiswal, R.K., Douglas, R., Mosca, J.D., Moorman, M.A., Simonetti, D.W., Craig, S., and Marshak, D.R. (1999). Multilineage potential of adult human mesenchymal stem cells. Science *284*, 143–147. https://doi.org/10.1126/SCIENCE.284.5411.143.

24. Naaldijk, Y., Johnson, A.A., Ishak, S., Meisel, H.J., Hohaus, C., and Stolzing, A. (2015). Migrational changes of mesenchymal stem cells in response to cytokines, growth factors, hypoxia, and aging. Exp. Cell Res. *338*, 97–104. https://doi.org/10.1016/J.YEXCR.2015.08.019.

25. Hass, R., Kasper, C., Böhm, S., and Jacobs, R. (2011). Different populations and sources of human mesenchymal stem cells (MSC): A comparison of adult and neonatal tissue-derived MSC. Cell Commun. Signal. *9*, 12. https://doi.org/10.1186/1478-811X-9-12.

26. Nowakowski, A., Drela, K., Rozycka, J., Janowski, M., and Lukomska, B. (2016). Engineered Mesenchymal Stem Cells as an Anti-Cancer Trojan Horse. Stem Cells Dev. *25*, 1513–1531. https://doi.org/10.1089/scd.2016.0120.

27. Kuroda, Y., and Dezawa, M. (2014). Mesenchymal stem cells and their subpopulation, pluripotent muse cells, in basic research and regenerative medicine. Anat. Rec. *297*, 98–110. https://doi.org/10.1002/ar.22798.

28. Dominici, M., Le Blanc, K., Mueller, I., Slaper-Cortenbach, I., Marini, F.C., Krause, D.S., Deans, R.J., Keating, A., Prockop, D.J., and Horwitz, E.M. (2006). Minimal criteria for defining multipotent mesenchymal stromal cells. The International Society for Cellular Therapy position statement. Cytotherapy *8*, 315–317. https://doi.org/10.1080/14653240600855905.

29. Uccelli, A., Moretta, L., and Pistoia, V. (2008). Mesenchymal stem cells in health and disease. Nat. Rev. Immunol. *8*, 726–736. https://doi.org/10.1038/nri2395.

30. Phinney, D.G., and Pittenger, M.F. (2017). Concise Review: MSC-Derived Exosomes for Cell-Free Therapy. Stem Cell. *35*, 851–858. https://doi.org/10.1002/STEM.2575.

31. Madrigal, M., Rao, K.S., and Riordan, N.H. (2014). A review of therapeutic effects of mesenchymal stem cell secretions and induction of secretory modification by different culture methods. J. Transl. Med. *12*, 260. https://doi.org/10.1186/s12967-014-0260-8.

32. Kou, M., Huang, L., Yang, J., Chiang, Z., Chen, S., Liu, J., Guo, L., Zhang, X., Zhou, X., Xu, X., et al. (2022). Mesenchymal stem cell-derived extracellular vesicles for immunomodulation and regeneration: a next generation therapeutic tool? Cell Death Dis. *13*, 580. https://doi.org/10.1038/s41419-022-05034-x.

33. Isik, B., Thaler, R., Goksu, B.B., Conley, S.M., Al-Khafaji, H., Mohan, A., Afarideh, M., Abumoawad, A.M., Zhu, X.Y., Krier, J.D., et al. (2021). Hypoxic preconditioning induces epigenetic changes and modifies swine mesenchymal stem cell angiogenesis and senescence in experimental atherosclerotic renal artery stenosis. Stem Cell Res. Ther. *12*, 240. https://doi.org/10.1186/S13287-021-02310-Z.

34. Asseng, S., Spänkuch, D., Hernandez-Ochoa, I.M., and Laporta, J. (2021). The upper temperature thresholds of life. Lancet Planet. Health *5*, e378–e385. https://doi.org/10.1016/S2542-5196(21)00079-6.

35. Moise, S., Byrne, J.M., El Haj, A.J., and Telling, N.D. (2018). The potential of magnetic hyperthermia for triggering the differentiation of cancer cells. Nanoscale *10*, 20519–20525. https://doi.org/10.1039/C8NR05946B.

36. Nir, D., Ribarski-Chorev, I., Shimoni, C., Strauss, C., Frank, J., and Schlesinger, S. (2022). Antioxidants Attenuate Heat Shock Induced Premature Senescence of Bovine Mesenchymal Stem Cells. Int. J. Mol. Sci. *23*, 5750. https://doi.org/10.3390/ijms23105750.

37. Gaete-Argel, A., Velásquez, F., Márquez, C.L., Rojas-Araya, B., Bueno-Nieto, C., Marín-Rojas, J., Cuevas-Zúñiga, M., Soto-Rifo, R., and Valiente-Echeverría, F. (2021). Tellurite Promotes Stress Granules and Nuclear SG-Like Assembly in Response to Oxidative Stress and DNA Damage. Front. Cell Dev. Biol. *9*, 200. https://doi.org/10.3389/FCELL.2021.622057.

38. Khan, A., Dou, J., Wang, Y., Jiang, X., Khan, M.Z., Luo, H., Usman, T., and Zhu, H. (2020). Evaluation of heat stress effects on cellular and transcriptional adaptation of bovine granulosa cells. J. Anim. Sci. Biotechnol. *11*, 25. https://doi.org/10.1186/S40104-019-0408-8.

39. Abdal Dayem, A., Lee, S., Y Choi, H., and Cho, S.G. (2018). The Impact of Adhesion Molecules on the In Vitro Culture and Differentiation of Stem Cells. Biotechnol. J. *13*, 1700575. https://doi.org/10.1002/BIOT.201700575.

40. Stopp, S., Bornhäuser, M., Ugarte, F., Wobus, M., Kuhn, M., Brenner, S., and Thieme, S. (2013). Expression of the melanoma cell adhesion molecule in human mesenchymal stromal cells regulates proliferation, differentiation, and maintenance of hematopoietic stem and progenitor cells. Haematologica *98*, 505–513. https://doi.org/10.3324/HAEMATOL.2012.065201.

41. Li, J., Labbadia, J., and Morimoto, R.I. (2017). Rethinking HSF1 in Stress, Development, and Organismal Health. Trends Cell Biol. *27*, 895–905. https://doi.org/10.1016/J.TCB.2017.08.002.

42. Su, K.H., and Dai, C. (2017). mTORC1 senses stresses: Coupling stress to proteostasis. Bioessays *39*, 1600268. https://doi.org/10.1002/BIES.201600268.

43. Johnson, S.C., Rabinovitch, P.S., and Kaeberlein, M. (2013). mTOR is a key modulator of ageing and age-related disease. Nature *493*, 338–345. https://doi.org/10.1038/NATURE11861.

44. Saxton, R.A., and Sabatini, D.M. (2017). mTOR Signaling in Growth, Metabolism, and Disease. Cell *168*, 960–976. https://doi.org/10.1016/J.CELL.2017.02.004.

45. Antonioli, E., Torres, N., Ferretti, M., Piccinato, C.A., and Sertie, A.L. (2019). Individual response to mTOR inhibition in delaying replicative senescence of mesenchymal stromal cells. PLoS One *14*, e0204784. https://doi.org/10.1371/JOURNAL.PONE.0204784.

46. Reimand, J., Isserlin, R., Voisin, V., Kucera, M., Tannus-Lopes, C., Rostamianfar, A., Wadi, L., Meyer, M., Wong, J., Xu, C., et al. (2019). Pathway enrichment analysis and visualization of omics data using g:Profiler, GSEA, Cytoscape and EnrichmentMap. Nat. Protoc. *14*, 482–517. https://doi.org/10.1038/S41596-018-0103-9.

47. Medvedeva, Y.A., Lennartsson, A., Ehsani, R., Kulakovskiy, I.V., Vorontsov, I.E., Panahandeh, P., Khimulya, G., Kasukawa, T.; FANTOM Consortium, and Drabløs, F. (2015). EpiFactors: a comprehensive database of human epigenetic factors andcomplexes. Database *2015*, bav067. https://doi.org/10.1093/DATABASE/BAV067.

48. Blake, J.A., Baldarelli, R., Kadin, J.A., Richardson, J.E., Smith, C.L., and Bult, C.J.; Mouse Genome Database Group (2021). Mouse Genome Database (MGD): Knowledgebase for mouse-human comparative biology. Nucleic Acids Res. *49*, D981–D987. https://doi.org/10.1093/NAR/GKAA1083.

49. Harikumar, A., and Meshorer, E. (2015). Chromatin remodeling and bivalent histone modifications in embryonic stem cells. EMBO Rep. *16*, 1609–1619. https://doi.org/10.15252/embr.201541011.

50. Noer, A., Lindeman, L.C., and Collas, P. (2009). Histone H3 modifications associated with differentiation and long-term culture of mesenchymal adipose stem cells. Stem Cells Dev. *18*, 725–736. https://doi.org/10.1089/scd.2008.0189.

51. Mas, G., Blanco, E., Ballaré, C., Sansó, M., Spill, Y.G., Hu, D., Aoi, Y., Le Dily, F., Shilatifard, A., Marti-Renom, M.A., and Di Croce, L. (2018). Promoter bivalency favors an open chromatin architecture in embryonic stem cells. Nat. Genet. *50*, 1452–1462. https://doi.org/10.1038/s41588-018-0218-5.

52. Bogliotti, Y.S., Wu, J., Vilarino, M., Okamura, D., Soto, D.A., Zhong, C., Sakurai, M., Sampaio, R.V., Suzuki, K., Izpisua Belmonte, J.C., and Ross, P.J. (2018). Efficient derivation of stable primed pluripotent embryonic stem cells from bovine blastocysts. Proc. Natl. Acad. Sci. USA *115*, 2090–2095. https://doi.org/10.1073/PNAS.1716161115.

53. Matsumura, Y., Nakaki, R., Inagaki, T., Yoshida, A., Kano, Y., Kimura, H., Tanaka, T., Tsutsumi, S., Nakao, M., Doi, T., et al. (2015). H3K4/H3K9me3 Bivalent Chromatin Domains Targeted by Lineage-Specific DNA Methylation Pauses Adipocyte Differentiation. Mol. Cell *60*, 584–596. https://doi.org/10.1016/J.MOLCEL.2015.10.025.

54. Bagath, M., Krishnan, G., Devaraj, C., Rashamol, V.P., Pragna, P., Lees, A.M., and Sejian, V. (2019). The impact of heat stress on the immune system in dairy cattle: A review. Res. Vet. Sci. *126*, 94–102. https://doi.org/10.1016/J.RVSC.2019.08.011.

55. Zhang, Y., Ling, L., Ajay D/O Ajayakumar, A., Eio, Y.M., van Wijnen, A.J., Nurcombe, V., and Cool, S.M. (2022). FGFR2 accommodates osteogenic cell fate determination in human mesenchymal stem cells. Gene *818*, 146199. https://doi.org/10.1016/J.GENE.2022.146199.

56. Khalid, A.B., Pence, J., Suthon, S., Lin, J., Miranda-Carboni, G.A., and Krum, S.A. (2021). GATA4 regulates mesenchymal stem cells via direct transcriptional regulation of the WNT signalosome. Bone *144*, 115819. https://doi.org/10.1016/J.BONE.2020.115819.

57. Fang, H., Kang, L., Abbas, Z., Hu, L., Chen, Y., Tan, X., Wang, Y., and Xu, Q. (2021). Identification of key Genes and Pathways Associated With Thermal Stress in Peripheral Blood Mononuclear Cells of Holstein Dairy Cattle. Front. Genet. *12*, 662080. https://doi.org/10.3389/FGENE.2021.662080.

58. van Velthoven, C.T.J., and Rando, T.A. (2019). Stem Cell Quiescence: Dynamism, Restraint, and Cellular Idling. Cell Stem Cell *24*, 213–225. https://doi.org/10.1016/J.STEM.2019.01.001.

59. Dalton, S., and Coverdell, P.D. (2015). Linking the cell cycle to cell fate decisions. Trends Cell Biol. *25*, 592–600. https://doi.org/10.1016/J.TCB.2015.07.007.

60. Gao, S.T., Ma, L., Zhou, Z., Zhou, Z.K., Baumgard, L.H., Jiang, D., Bionaz, M., and Bu, D.P. (2019). Heat stress negatively affects the transcriptome related to overall metabolism and milk protein synthesis in mammary tissue of midlactating dairy cows. Physiol. Genomics *51*, 400–409. https://doi.org/10.1152/PHYSIOLGENOMICS.00039.2019.

61. Roth, Z. (2020). Reproductive physiology and endocrinology responses of cows exposed to environmental heat stress - Experiences from the past and lessons for the present. Theriogenology *155*, 150–156. https://doi.org/10.1016/J.THERIOGENOLOGY.2020.05.040.

62. Choudhery, M.S. (2021). Strategies to improve regenerative potential of mesenchymal stem cells. World J. Stem Cells *13*, 1845–1862. https://doi.org/10.4252/WJSC.V13.I12.1845.

63. Smedley, D., Haider, S., Ballester, B., Holland, R., London, D., Thorisson, G., and Kasprzyk, A. (2009). BioMart - Biological queries made easy. BMC Genom. *10*, 22. https://doi.org/10.1186/1471-2164-10-22.

64. Quinlan, A.R., and Hall, I.M. (2010). BEDTools: a flexible suite of utilities for comparing genomic features. Bioinformatics *26*, 841–842. https://doi.org/10.1093/BIOINFORMATICS/BTQ033.

65. Heinz, S., Benner, C., Spann, N., Bertolino, E., Lin, Y.C., Laslo, P., Cheng, J.X., Murre, C., Singh, H., and Glass, C.K. (2010). Simple combinations of lineage-determining transcription factors prime cis-regulatory elements required for macrophage and B cell identities. Mol. Cell *38*, 576–589. https://doi.org/10.1016/J.MOLCEL.2010.05.004.

66. Shannon, P., Markiel, A., Ozier, O., Baliga, N.S., Wang, J.T., Ramage, D., Amin, N., Schwikowski, B., and Ideker, T. (2003). Cytoscape: A Software Environment for Integrated Models of Biomolecular Interaction Networks. Genome Res. *13*, 2498–2504. https://doi.org/10.1101/GR.1239303.

67. Martin, M. (2011). Cutadapt removes adapter sequences from high-throughput sequencing reads. EMBnet. J. *17*, 10–12.

68. Bindea, G., Mlecnik, B., Hackl, H., Charoentong, P., Tosolini, M., Kirilovsky, A., Fridman, W.H., Pagès, F., Trajanoski, Z., and Galon, J. (2009). ClueGO: a Cytoscape plug-in to decipher functionally grouped gene ontology and pathway annotation networks.

Bioinformatics *25*, 1091–1093. https://doi.org/10.1093/BIOINFORMATICS/BTP101.

69. Love, M.I., Huber, W., and Anders, S. (2014). Moderated estimation of fold change and dispersion for RNA-seq data with DESeq2. Genome Biol. *15*, 550. https://doi.org/10.1186/S13059-014-0550-8.

70. Subramanian, A., Tamayo, P., Mootha, V.K., Mukherjee, S., Ebert, B.L., Gillette, M.A., Paulovich, A., Pomeroy, S.L., Golub, T.R., Lander, E.S., and Mesirov, J.P. (2005). Gene set enrichment analysis: A knowledge-based approach for interpreting genome-wide expression profiles. Proc. Natl. Acad. Sci. USA *102*, 15545–15550. https://doi.org/10.1073/PNAS.0506580102.

71. Mudunuri, U., Che, A., Yi, M., and Stephens, R.M. (2009). bioDBnet: the biological database network. Bioinformatics *25*, 555–556. https://doi.org/10.1093/BIOINFORMATICS/BTN654.

72. Reimand, J., Arak, T., Adler, P., Kolberg, L., Reisberg, S., Peterson, H., and Vilo, J. (2016). g:Profiler-a web server for functional interpretation of gene lists (2016 update). Nucleic Acids Res. *44*, W83–W89. https://doi.org/10.1093/NAR/GKW199.

73. Hulsen, T., de Vlieg, J., and Alkema, W. (2008). BioVenn - A web application for the comparison and visualization of biological lists using area-proportional Venn diagrams. BMC Genom. *9*, 488. https://doi.org/10.1186/1471-2164-9-488.

74. Anders, S., Pyl, P.T., and Huber, W. (2015). HTSeq—a Python framework to work with high-throughput sequencing data. Bioinformatics *31*, 166–169. https://doi.org/10.1093/BIOINFORMATICS/BTU638.

75. Robinson, J.T., Thorvaldsdóttir, H., Winckler, W., Guttman, M., Lander, E.S., Getz, G., and Mesirov, J.P. (2011). Integrative Genomics Viewer. Nat. Biotechnol. *29*, 24–26. https://doi.org/10.1038/NBT.1754.

76. Kanehisa, M., and Goto, S. (2000). KEGG: Kyoto Encyclopedia of Genes and Genomes. Nucleic Acids Res. *28*, 27–30. https://doi.org/10.1093/NAR/28.1.27.

77. Belinky, F., Nativ, N., Stelzer, G., Zimmerman, S., Iny Stein, T., Safran, M., and Lancet, D. (2015). PathCards: multi-source consolidation of human biological pathways. Database *2015*, bav006. https://doi.org/10.1093/DATABASE/BAV006.

78. García-Alcalde, F., Okonechnikov, K., Carbonell, J., Cruz, L.M., Götz, S., Tarazona, S., Dopazo, J., Meyer, T.F., and Conesa, A. (2012). Qualimap: evaluating next-generation sequencing alignment data. Bioinformatics *28*, 2678–2679. https://doi.org/10.1093/BIOINFORMATICS/BTS503.

79. Croft, D., O'Kelly, G., Wu, G., Haw, R., Gillespie, M., Matthews, L., Caudy, M., Garapati, P., Gopinath, G., Jassal, B., et al. (2011). Reactome: a database of reactions, pathways and biological processes. Nucleic Acids Res. *39*, D691–D697. https://doi.org/10.1093/NAR/GKQ1018.

80. Dobin, A., Davis, C.A., Schlesinger, F., Drenkow, J., Zaleski, C., Jha, S., Batut, P., Chaisson, M., and Gingeras, T.R. (2013). STAR: ultrafast universal RNA-seq aligner. Bioinformatics *29*, 15–21. https://doi.org/10.1093/BIOINFORMATICS/BTS635.

81. Szklarczyk, D., Gable, A.L., Lyon, D., Junge, A., Wyder, S., Huerta-Cepas, J., Simonovic, M., Doncheva, N.T., Morris, J.H., Bork, P., et al. (2019). STRING v11: protein–protein association networks with increased coverage, supporting functional discovery in genome-wide experimental datasets. Nucleic Acids Res. *47*, D607–D613. https://doi.org/10.1093/NAR/GKY1131.

82. Uccelli, A., Moretta, L., and Pistoia, V. (2008). Mesenchymal stem cells in health and disease. Nat. Rev. Immunol. *8*, 726–736.

83. Toupadakis, C.A., Wong, A., Genetos, D.C., Cheung, W.K., Borjesson, D.L., Ferraro, G.L., Galuppo, L.D., Leach, J.K., Owens, S.D., and Yellowley, C.E. (2010). Comparison of the osteogenic potential of equine mesenchymal stem cells from bone marrow, adipose tissue, umbilical cord blood, and umbilical cord tissue. Am. J. Vet. Res. *71*, 1237–1245. https://doi.org/10.2460/AJVR.71.10.1237.

84. Rosen, B.D., Bickhart, D.M., Schnabel, R.D., Koren, S., Elsik, C.G., Tseng, E., Rowan, T.N., Low, W.Y., Zimin, A., Couldrey, C., et al. (2020). De novo assembly of the cattle reference genome with single-molecule sequencing. GigaScience *9*, giaa021. https://doi.org/10.1093/GIGASCIENCE/GIAA021.

85. Okonechnikov, K., Conesa, A., and García-Alcalde, F. (2016). Qualimap 2: advanced multi-sample quality control for high-throughput sequencing data. Bioinformatics *32*, 292–294. https://doi.org/10.1093/BIOINFORMATICS/BTV566.

86. Youlten, S.E., Kemp, J.P., Logan, J.G., Ghirardello, E.J., Sergio, C.M., Dack, M.R.G., Guilfoyle, S.E., Leitch, V.D., Butterfield, N.C., Komla-Ebri, D., et al. (2021). Osteocyte transcriptome mapping identifies a molecular landscape controlling skeletal homeostasis and susceptibility to skeletal disease. Nat. Commun. *12*, 2444. https://doi.org/10.1038/S41467-021-22517-1.

STAR★METHODS

KEY RESOURCES TABLE

REAGENT or RESOURCE	SOURCE	IDENTIFIER
Antibodies		
G3BP1 antibody	Invitrogen	Cat# PA5-82129; RRID:AB_2789290
Phalloidin-iFluor 532 Reagent	Abcam	Cat# ab176755
Secondary antibody of Alexa Flour 488 goat anti-rabbit	Invitrogen	Cat# A-11070; RRID:AB_142134
Biological samples		
MSC extracted from umbilical cords of cattle	Holstein cows	NA
Chemicals, peptides, and recombinant proteins		
3-isobutyl-1-methyl-xanthine	Sigma	Cat# I5879
Alcian blue	Sigma-Aldrich	Cat# A5268
Ascorbic acid-2-phosphate	Sigma	Cat# A8960
Bodipy 493/503	Invitrogen	Cat# D3922
Collagenase Type I	Invitrogen	Cat# 17100017
Collagenase Type II	Sigma	Cat# C6885
Dexamethasone	Sigma	Cat# D4902
DMEM low glucose	Gibco or Biological Industries	Cat# 31885023 or 04-001-1A
DMSO	Sigma-Aldrich	Cat# W387520
Elastase Type IV	Sigma	Cat# E0258
Fetal Bovine Serum (FBS)	Biological Industries	Cat# 04-001-1A
Glutamine	Biological Industries	Cat# 03-020-1B
Hyaluronidase Type I-S	Sigma	Cat# H3506
Indomethacin	Sigma	Cat# I7378
Insulin-Transferrin-Selenium	Gibco	Cat# 41400-045
Penicillin-streptomycin solution	Biological Industries	Cat# 03-031-1B
Recombinant human (rh) insulin	Sigma	Cat# I2643
Transforming Growth Factor-beta 1 (TGFβ1)	PeproTech	Cat# 100-21C
β –glycerophosphate	Sigma	Cat# G9422
Critical commercial assays		
PureLink RNA Minikit	Invitrogen	Cat# 12183018A
qScriptTM cDNA Synthesis Kit	Quanta-bio	Cat# 95047-100
Fast SYBR Green Master Mix	Applied Biosystem	Cat# 4385614
Deposited data		
Raw and analyzed data. See Table S6.	This paper	GEO: GSE214467
Bovine reference genome: Bos_taurus.ARS-UCD1.2		https://www.ensembl.org/info/data/ftp/index.html
Oligonucleotides		
Primers for qRT-PCR, See Table S8	This paper	N/A
Software and algorithms		
BEDTools (v2.30.0)	Quinlan and Hall,[63]	
bioDBnet	Mudunuri,[64]	

(*Continued on next page*)

Continued

REAGENT or RESOURCE	SOURCE	IDENTIFIER
BioVenn	Hulsen,[65]	https://www.biovenn.nl/index.php
ClueGO (v2.5.7)	Bindea,[66]	
Cutadapt (v0.13.5)	Martin,[67]	
Cytoscape	Shannon,[68]	http://www.cytoscape.org/
DESeq2 package	Love,[69]	
Enrichment Analysis (GSEA) software (v4.1.0)	Subramanian,[70]	http://software.broadinstitute.org/gsea/
Ensembl BioMart	Smedley,[71]	
EpiFactors Database	Medvedeva,[47]	https://epifactors.autosome.org/
FastQC (v0.11.9)		https://www.bioinformatics.babraham.ac.uk/projects/fastqc/
g:Profiler	Reimand,[72]	https://biit.cs.ut.ee/gprofiler/
GraphPad Prism (v.8.4.3 for windows)	Graphpad	https://www.graphpad.com/scientificsoftware/prism/
HOMER (v4.11)	Heinz,[73]	
HTSeq (v0.13.5)	Anders,[74]	
Inkscape Project (2020)		https://inkscape.org/
Integrative Genomics Viewer (IGV) (v2.12.0)	Robinson,[75]	https://software.broadinstitute.org/software/igv
KEGG pathway database	Kanehisa & Goto,[76]	https://www.genome.jp/kegg/pathway.html
MGD (Mouse Genome Database)	Blake,[48]	http://www.informatics.jax.org/vocab/gene_ontology/
PathCards (v5.7.551.0)	Belinky[77]	https://pathcards.genecards.org/
QualiMap (v2.2.1)	García-Alcalde,[78]	http://qualimap.conesalab.org/
Reactome	Croft,[79]	
RStudio (v2022.07.1+554)	R Foundation for Statistical Computing	https://www.rstudio.com/
STAR (v2.7.1a)	Dobin,[80]	
STRING	Szklarczyk,[81]	https://string-db.org/
The Graeber lab online hypergeometric calculator 2009 ©		https://systems.crump.ucla.edu/hypergeometric/

RESOURCE AVAILABILITY

Lead contact

Further information and requests for resources and reagents should be directed to the lead contact, Dr. Sharon Schlesinger (sharon.shle@mail.huji.ac.il).

Materials availability

This study did not generate new unique reagents.

Data and code availability

- The datasets supporting the conclusions of this article are available in the GEO repository, GSE214467 study. Final DESeq2 analysis of this data is available in Table S6. In addition, some datasets supporting the conclusions of this article are included within the article additional files, Tables S3, S4, S5, and S7.
- This paper does not report original code.
- Any additional information required to reanalyze the data reported in this paper are available from the lead contact upon request.

EXPERIMENTAL MODEL AND SUBJECT DETAILS

This study used MSC extracted from umbilical cords (UC) of Holstein cows from abattoirs located in the north of Israel. Three MSCs lines (two female and one male) were used for this study. The two female lines were verified previously.[15,36] See cell culture and cell characterization sections in method details for further

information. The procedures of isolated UC-MSCs were conducted abiding by the Institutional Animal Care and Use Committee (IAACUC) of the Israel Ministry of Agriculture and Rural Development, permit #11380.

METHOD DETAILS

Cell culture

Bovine mesenchymal stem cells were isolated, cultured and characterized based on generally accepted criteria[28,82] as we have previously reported.[15,36] Briefly, umbilical cords (UCs) of Holstein dairy cows were obtained from abattoirs located in the north of Israel. In the lab, the UCs were digested and plated as previously described in.[83] In short, the UC was first soaked in 70% ethanol for 30 s and then soaked in Dulbecco's phosphate-buffered saline (DPBS) containing 3% Penicillin-Streptomycin, 1% Gentamycin and 1%, Amphotericin b to prevent contamination further down the line. Blood vessels were removed from the tissue, the tissue was minced into small pieces and incubated in a 37°C water bath for 1 hour in a digestion cocktail containing 0.4% (w/v) Collagenase Type I, 0.4% (w/v) Collagenase Type II, 0.008% (w/v) Elastase Type IV, and 0.2% (w/v) Hyaluronidase. Following digestion, cells were separated from the remaining tissue by filtration through a 70 μm nylon filter and washed several times by centrifugation in DPBS. Cells were plated in a low glucose Dulbecco's Modified Eagle's Medium (Gibco - 31885-023 or Biological Industries (BI) - 04-001-1A) containing 10% fetal bovine serum (FBS) (BI, 04-001-1A), penicillin-streptomycin solution 1% (BI, 03-031-1B), Glutamine 1% (BI, #03-020-1B) and cryopreserved at different passages using FBS with 10% DMSO (Sigma-Aldrich, W387520). The media was changed every 3-4 days and all cells were cultured in a humidified incubator with a controlled environment of 5% CO2 and a temperature of 37°C, unless mentioned otherwise. The procedures of isolated UC-MSCs were conducted abiding by the Institutional Animal Care and Use Committee of the Israel Ministry of Agriculture and Rural Development, permit #11380.

Cell characterization

Three bovine MSCs lines were used in this study. Two were previously examined and verified[15,36] and the third was examined and verified in this study (Figure S1) before subsequent heat shock experiments. One line was used for the RNA-seq experiment, while all three lines were used for Real-Time PCR (RT-qPCR), differentiation and further examinations. Differentiation potential was examined for osteoblasts, adipocytes, and chondrocytes fates. Regarding heat shock experiments, on day 3 following treatments, differentiation protocol was initiated. To induce osteogenic differentiation media containing LG-DMEM, 10% FCS, 10−7M dexamethasone, 100 μM ascorbic acid-2-phosphate and 10 mM β−glycerophosphate was changed every 3 days and after 10 days osteogenic differentiation was assessed using alizarin red S staining. For adipogenic differentiation, the cells were cultured in LG-DMEM, 10% FBS, 10−6M dexamethasone, 0.5 mM 3-isobutyl-1-methyl-xanthine, 0.2 mM indomethacin, and 10μg/mL recombinant human (rh) insulin and differentiation was assessed by staining with 4,4-difluoro-1,3,5,7,8-pentamethyl-4-bora-3a,4a-diaza-s-indacene (Bodipy 493/503, Invitrogen), added with 5μg/mL DAPI (Sigma). To promote chondrogenic differentiation, cells were cultured for 3 weeks in Dulbecco's Modified Eagle Medium:Nutrient Mixture F-12 (DMEM/F-12) media supplemented with 5% FBS, 100 IU/mL penicillin, 0.1mg/mL streptomycin, 2 mM L-glutamine (Biological Industries), 1% Insulin-Transferrin-Selenium (ITS-G, Gibco) and 10ng/mL Transforming Growth Factor-beta 1 (TGFβ1, PeproTech). Differentiation was assessed by staining with 0.6% Alcian Blue (Sigma-Aldrich). Following staining, plates were taken to microscopic evaluation, using EVOS FL Auto imaging system (ThermoFisher Scientific). Negative control was carried out using stained cells grown without differentiation media. All the experiments described were done on cells in passages 2-4, and at least 3 biological replicas were used unless specified otherwise.

Cell death quantification using Propidium Iodide (PI)

For quantification of cell death in culture, cells were harvested by trypsinization, washed with PBS, and resuspended in 10 g/mL PI for 5 min on ice. The percentage of live/dead cells was determined within 1 h of staining by flow cytometry (CytoFLEX, Beckman Coulter, Indianapolis, IN, USA). 10,000 events were collected per sample. At least three biological repeats were used for each treatment. Data analysis was performed using Flow-Jo software.

Heat-shock induction

MSCs at early passages (P2–P4) were seeded in 6-well plates (Costar, 3516) at different concentrations to allow similar confluence at the end of the experiment, as shown in Table S2. The cells were incubated for 24 h in normal conditions before treatment onset (time 0).

Cell counting

Following the HS, the cells were washed with Dulbecco's Phosphate Buffered Saline (BI, 02-021-IA) and trypsinized (BI, 03-053-1A). 6μL of trypsinized cells were mixed with 6μL of trypan-blue (Sigma, T8154), loaded into an appropriate slide, and counted using an automated cell counter (TC20, Bio-Rad Laboratories Hercules, CA, USA). Three to five biological repeats were performed.

Population doubling time

Starting from passage 2, three replicas of 40 K cells per well were plated in 6-well plates. This process was repeated every 3-4 days for 10 passages. Population doubling (PD) time was calculated using the formula PDt = SQRT(N/N0)/t (where SQRT, N, N0, and t are the square root, final cell numbers, the initial cell number, and the cell time in the culture, respectively). Three biological replicas were used for each time point.

Immunofluorescence

For stress granules immunofluorescence staining following HS treatment, the cells were washed once with PBS and fixed with 4% paraformaldehyde for 10 min at room temperature. Then, cells were washed three times with PBS, permeabilized with 0.2% Triton for 5 min, and washed again with PBS. For SGs markers staining, cells were incubated with blocking media containing 1% fetal calf serum (FCS) and 0.1% saponin for 2 hours in room temperature together with G3BP1 antibody (PA5-82129, Invitrogen). Then, cells were washed three times with PBS followed by incubation (1% FCS, 0.1% saponin) for 1 room temperature with secondary antibody of Alexa Flour 488 goat anti-rabbit (A11070 Invitrogen), Phalloidin-iFluor 532 Reagent (AB-ab176755) and DAPI. Finally, cells were washes three times in PBS, and mounted on glass slides using Fluorescent Mounting Medium (GBI Labs, E18-18). Inverted Nikon ECLIPSE TI-DH Florescent Microscope was used, and image acquisition was carried out with a 60X objective.

RNA-sequencing

Total RNA from the heat shocked cells was extracted via PureLink RNA Minikit (Invitrogen, 12183018A). RNA concentrations were measured using a NanoDrop ND1000- spectrophotometer (NanoDrop Technologies) and the quality of extracted RNA was confirmed (RNA integrity number (RIN) > 9) using an Agilent2100 Bioanalyzer before further processing. Library preparation was done using the INCPM mRNA library of the Weizmann Institute, Rehovot. The quality of cDNA libraries was determined using a tape-station. Sequencing was done using Nextseq Illumina in the INCPM of Weizmann Institute, with single-end reads of 75 bp. Sequencing was done on 14 samples from the same MSC line as in,[15] and after initial quality analysis one sample was removed and we were left with 13 samples to perform the in-depth analysis: 3 biological replicas for ShortNT, ShortHS and LongHS treatments, and 2 biological replicas for LongNT and ShortHS_Recovery treatments.

Data analysis

Following sequencing, reads were trimmed for adaptors and poly A using Cutadapt v.0.13.5,[67] checked for quality by FastQC 0.11.9, mapped to most recent annotated bovine genome Bos_taurus.ARS-UCD1.2[84] and counted using STAR 2.7.1a[80] and HTSeq 0.13.5[74] accordingly. Further quality control of alignment sequencing data was done using Integrative Genomics Viewer (IGV) 2.12.0[75] and QualiMap v.2.2.1.[78,85] Normalization of the counts and differential expression analysis were performed using DESeq2 package in RStudio.[69] Total of 27,607 genes were sequenced. Genes with less than 5 counts in total per all treatments were removed, and we left with 16,595 genes for further downstream analyses (Table S6). PCA, hierarchical and K-means clustering as well as other data visualizations, were performed using Rstudio v2022.07.1.

Functional enrichment analysis was conducted using both ranked gene list analyses using Gene Set Enrichment Analysis (GSEA) software version 4.1.0[70] and DEGs list analysis using g:Profiler[72] version e103_e.g.,50_p15_eadf141 and ClueGO v2.5.7 a Cytoscape plug-in[66,68] with default parameters. GSEA was used for Hallmark genes set and Gene Ontology (GO) enrichments, while g:Profiler and CluGo were used for GO, Kyoto Encyclopedia of Genes and Genomes (KEGG) and Reactome pathways analysis. KEGG pathway maps were downloaded from KEGG pathway database.[76] Epigenetic complexes analysis was performed using the EpiFactors Database[47] as well GO annotations of the MGD (Mouse Genome Database).[48] The cytokine pathway list was taken from PathCards v5.7.551.0.[77] Bivalent genes enrichment was done by comparing our genes lists to ESCs bivalent genes of mouse and cattle as well as to MSCs

bivalent genes of mouse.[51–53] For detailed information on data analysis see bioinformatic analysis supplementary.

RNA extraction, reverse transcription, and Real-time PCR

RNA extraction from cells was carried out using GenElute™ Total RNA Purification Kit (Sigma, RNB100-50RXN). RNA was then reverse-transcribed into cDNA using qScriptTM cDNA Synthesis Kit (Quanta-bio, 95047-100). Real-Time PCR (RT-qPCR) reactions were performed using Fast SYBR Green Master Mix (Applied Biosystem, 4385614) in an ABI Step-One Plus Real-Time PCR system. All primers were verified by standard curve evaluation and are shown in Table S8. Primers for expression analysis were designed on exon-exon junctions and a -RT control was performed each time. Relative mRNA fold change was calculated with the ΔΔCT method, using 1-2 control genes (PSMB2 and RPS9) as reference.

QUANTIFICATION AND STATISTICAL ANALYSIS

GraphPad Prism version 8.4.3 for windows, GraphPad Software, San Diego, California USA, was used for statistical analysis and visualization of RT-qPCR. $p < 0.05$ was considered statistically significant. Bivalent genes (Figure 4) as well specific pathways (Figure 5) enrichment analysis was calculated using the Graeber lab online hypergeometric calculator 2009 © (https://systems.crump.ucla.edu/hypergeometric/index.php).[86]